The Journal of Physical Chemistry A

 VOLUME 101, NUMBER 14, APRIL 3, 1997

# ARTICLES

## Time-Resolved Laser-Induced Fluorescence Study of Photoinduced Electron Transfer at the Water/1,2-Dichloroethane Interface

**Robert A. W. Dryfe,[†] Zhifeng Ding,[†] R. Geoffrey Wellington,[†] Pierre F. Brevet,[†] Alexander M. Kuznetzov,[‡] and Hubert H. Girault*,[†]**

*Laboratoire d'Electrochimie, Département de Chimie, Ecole Polytechnique Fédérale de Lausanne, CH-1015 Lausanne, Switzerland, and Frumkin Institute of Electrochemistry, Moscow 117971, Russia*

*Received: October 3, 1996; In Final Form: February 3, 1997*[⊗]

Time-resolved laser-induced fluorescence in total internal reflection mode has been used to monitor the lifetimes of excited species located within the evanescent wave on the aqueous side of the water/1,2-dichloroethane interface, in the presence of varying concentrations of quencher molecules in the adjacent organic phase. The aqueous chromophore used was europium(III), with anthracene being employed as the organic quencher. The kinetic data are obtained from analysis of the relevant mass-transfer regime. The heterogeneous electron transfer rate constant between the two species was found to be $1.9 \times 10^{-4}$ m$^4$ mol$^{-1}$ s$^{-1}$.

### Introduction

Electron transfer across the interface between two immiscible liquids has received a great deal of attention in recent years, both from a theoretical and an experimental standpoint.[1,2] This growth of interest perhaps stems from the realization that the liquid−liquid interface is useful as a simplified model of biological membranes, as well as being of relevance to phenomena such as solvent extraction.[3] The relative paucity of data on electron transfer at the liquid−liquid interface—in comparison to that at the metal−electrolyte and semiconductor−electrolyte interfaces—is now being addressed, although there have been few studies of photoinduced phenomena at this interface. Photoinduced electron transfer across the semiconductor−electrolyte interface has been widely studied over the past few decades, although corresponding studies at the metal−electrolyte interface had led to the conclusion that solution phase excited state species are quenched by the metallic surface.[4] At the interface between immiscible liquids, heterogeneous "dark" electron transfer is now well characterized with recent reports attempting to quantify the rates of such processes to allow comparison with the predictions of the theories of Marcus.[5] Likewise, photoinduced electron transfer events have been widely studied in "bulk" solution.[6] Studies at the interface between two immiscible electrolyte solutions (ITIES) have included the measurement of photocurrents associated with the quenching of the sensitizer tris(2,2′-bipyridine)ruthenium ($Ru(bpy)_3^{2+}$), dissolved in one of the liquid phases, by a quenching species located in the other phase.[7−9] A photoelectrochemical effect at the water/1,2-dichloroethane interface has been observed by Kotov *et al.*, but this was attributed to the transfer of a photochemically generated species rather than direct electron transfer.[10] In a similar vein, Samec and co-workers have reported the photochemical transfer of tetraaryl anions across the ITIES.[11] In this paper we report results obtained from an investigation of photoinduced heterogeneous electron transfer, the heterogeneity resulting from the presence of the liquid−liquid interface.

The investigative tool chosen was nanosecond pulsed laser

* E-mail: girault@icp.dc.epfl.ch. FAX: (+41) 21 693 3667.
† Ecole Polytechnique Fédérale de Lausanne.
‡ Frumkin Institute of Electrochemistry.
⊗ Abstract published in *Advance ACS Abstracts,* March 15, 1997.

S1089-5639(96)03043-5 CCC: $14.00 

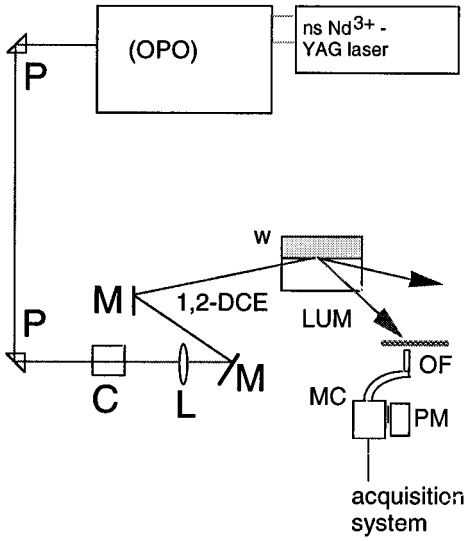


**Figure 1.** Schematic diagram of the quartz cell used in total internal reflection (TIR) mode for spectroscopic studies of charge transfer at the liquid−liquid interface. The abbreviations are P, prism; OPO, optical parametric oscillator; M, mirror; C, second-harmonic crystal; L, lens; LUM, luminescence; W, water; 1,2-DCE, 1,2-dichloroethane; MC, monochromator; OF, optical filter; PM, photomultiplier.

spectroscopy, with time-resolved luminescence used to access the lifetimes of the excited state species in the solution phase. Under normal circumstances, the bulk signal swamps the interfacial response; thus no information can be gleaned on processes occurring at the latter. However, in the experiments described below, the laser beam was used in total internal reflection (TIR) mode,[12] whereby the incident light beam approaches the liquid−liquid interface through the organic phase at an angle greater than the critical angle; thus its intensity in the aqueous phase decays exponentially with distance from the interface. This leads to an evanescent wave typically around 100 nm thick, which produces a narrow "diffusion layer" of excited state species in the aqueous phase, and thus the interfacial characteristics of the luminescent signal are enhanced.

The europium(III) cation was chosen as the excited state aqueous phase species, principally because of its long lifetime (hundreds of microseconds), which militates for the observation of any interfacial effect as the chances of the ion diffusing to the interface before it relaxes to its electronic ground state are increased.[13] Earlier spectroscopic studies of a similar type, using the shorter lived excited state of the sensitizer $Ru(bpy)_3^{2+}$ with tetracyanoquinodimethane as a quencher, were unable to measure heterogeneous electron transfer rate constants.[14] The analysis below will rationalize this observation, the main argument being that the TIR technique is only applicable to long-lived excited states. For this reason a species with a long-lived excited state, with no tendency to partition to the oil phase, was used as the sensitizing species in the present study.

## Experimental Section

**Spectroscopic Techniques.** The experimental apparatus for time-resolved TIR spectroscopy is shown schematically in Figure 1. Flash photolysis experiments were carried out with a Q-switched $Nd^{3+}$:YAG laser (Quanta-Ray Model 170-10) with 5-ns pulse duration and a frequency of 10 Hz. The third harmonic ($\lambda = 355$ nm) with an energy of 300 mJ/pulse was passed through an optical parametric oscillator (OPO) (Quanta-Ray, MOPO-710) to give monochromatic light of a wavelength corresponding to twice the absorption maximum of the europium ion in water (786 nm). Light from the OPO was frequency doubled using a potassium dihydrogen phosphate crystal (Fuzhou Casix Optronix Inc, Fuzhou, PR China) to give the wavelength corresponding to the maximum absorption band of the cation[13] and directed by way of the optics shown in Figure 1 through the quartz wall of the spectroelectrochemical cell, impinging on the interface from the dichloroethane (DCE) phase. The incidence angle of the beam with respect to the DCE/water interface was adjusted so that the excitation beam, focused at the interface, was totally reflected. The critical angle for the DCE/water interface, beyond which all light is reflected rather than refracted, is 67.56° when both phases consist of pure solvents. The experiment was carried out at an incidence angle set to about 79°. In this case the characteristic penetration depth is given by

$$\zeta = \frac{\lambda}{2\pi} \frac{1}{n_1\sqrt{\sin^2\theta - n_2^2/n_1^2}} \qquad (1)$$

where $\lambda$ is the wavelength of the incident light, $\theta$ is the angle of incidence, and $n_1$, $n_2$ are the optical indices of the DCE and the water phase, respectively. For example, at an angle of incidence of 79°, the penetration depth $\zeta$ is 130 nm for the wavelength of light employed.

The luminescence from the europium ions was collected through the side of the cell as shown in Figure 1. The luminescence was first filtered using an OG515 filter and then passed through a monochromator to a custom-made photomultiplier tube (R928, constructed in house), to amplify the emission maximum (615 nm).

Time resolution was achieved with a high-bandwidth (500 MHz) oscilloscope (Tektronix, Model TDS520A), the data being down-loaded to a microcomputer for further processing. A Perkin-Elmer luminescence spectrometer (Model LS 50 B) was used for absorption/emission spectroscopy.

**Chemicals.** Europium(III) was obtained as a 99.9% pure chloride salt from Johnson Matthey GmbH (Karlsruhe, Germany). Anthracene (99.9% purity) was obtained from Aldrich-Chemie (Steinheim, Germany). Bis(triphenylphosphoranylidene)−ammonium chloride (purum) and lithium sulfate (purum) were also supplied by Fluka. The organic solvents used were "extra pure" grade 1,2-dichloroethane (DCE) and "UV spectroscopy" grade acetone, obtained from Merck Suisse SA (Geneva, Switzerland). Water was purified by reverse osmosis followed by ion exchange (Milli-Q SP Reagent Water System).

**Theory.** The competing physical processes that control the fate of the excited state europium ion are described mathematically, and the resultant equations solved to predict the magnitude of any quenching effect. Mass transport occurs by diffusion of the excited ions to the interface, a process that competes with their luminescent decay, as illustrated in Figure 2. The initial concentration profile of excited state species is assumed to decay exponentially as discussed in the introductory section. Thus

$$c(x)_{t=0} = A\exp(\gamma x) \qquad (2)$$

where $t = 0$ corresponds to the time where the light pulse is incident on the interface, arriving at an angle of incidence that gives a penetration depth, $1/\gamma$, defined in eq 1 accounting for the intensity variation of the exciting beam as a function of distance and sensitizer concentration in a manner analogous to the Beer−Lambert law, and $A$ is a pre-exponential term. In fact the extinction coefficient of europium is so low that the exponential decay in the excited state concentration profile with distance can be treated solely in terms of the decay of the reflected wave due to its inability to propagate through the water. Note that the $x$ coordinate values are taken as being negative

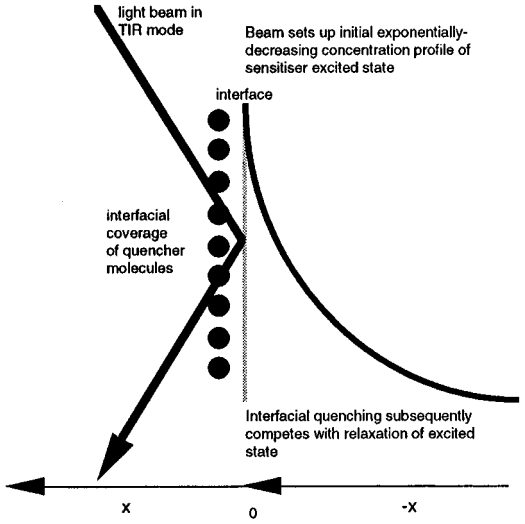


**Figure 2.** Illustration of the competing physical processes assumed to occur at the liquid−liquid interface.

on the aqueous side of the interface and positive on the organic phase (quencher) side.

Mathematically, the overall mass-transport equation for the excited state species can be written as

$$\frac{\partial c(x)}{\partial t} = D\frac{\partial^2 c}{\partial x^2} - k_f c(x) \tag{3}$$

where $D$ is the diffusion coefficient of the excited state and $k_f$ is the first order rate constant for loss of the excited state by luminescence. The rate constant, $k_f$ , is simply the inverse of the excited state lifetime, $\tau_0$, of the sensitizer species.

The excited state is quenched only at the interface: the quenching is a second-order process that is dependent on both the interfacial concentration of the quencher and the interfacial concentration of the sensitizer as defined by the above equations. The interfacial boundary condition can be written as

$$D\left(\frac{\partial c(x)}{\partial t}\right)_{x=0} = k_{12} c_q c(0) \tag{4}$$

where $k_{12}$ is the second-order quenching rate constant, $c_{(0)}$ is the concentration of excited state sensitizer located at the interface, and $c_q$ is the quencher concentration.

These equations define the model represented schematically in Figure 2, and their solution demonstrates the effect of the various physical parameters on the observed excited state lifetime, $\tau$, of the sensitizer species. The solution of these equations was performed using the method described below.

**Analytical Solution.** The above system of equations is transformed into Laplace space, which then enables the concentration profile of the excited state to be calculated as a function of time. Integration of the concentration profile leads to the signal intensity at that time, and hence the decay curve can be simulated to give the excited state lifetime under the designated conditions.

The Laplace transform of the second-order differential equation (3) is

$$\frac{\partial^2 \bar{c}(x,p)}{\partial x^2} - u^2(p)\,\bar{c}(x,p) + B\exp(\gamma x) = 0 \tag{5}$$

and the boundary condition (4) is given by

$$\frac{\partial \bar{c}(x,p)}{\partial x} + \kappa \bar{c}(x,p) = 0 \tag{6}$$

where

$$u^2(p) = \frac{p + k_f}{D} \qquad B = \frac{A}{D} \qquad \kappa = \frac{k_{12} c_q}{D} \tag{7}$$

The solution of this problem then reads

$$\bar{c}(x,p) = B\left[\frac{\kappa + \gamma}{(\gamma^2 - u^2)(\kappa + u)}\exp(ux) + \frac{1}{u^2 - \gamma^2}\exp(\gamma x)\right] \tag{8}$$

The concentration must be integrated over the whole evanescent wave to give the signal intensity,

$$\bar{N}(p) = \frac{B}{\gamma}\left[\frac{\gamma}{\kappa(\kappa - \gamma)(u + \kappa)} + \frac{\gamma + \kappa}{\kappa\gamma u} + \frac{\kappa}{\gamma(\gamma - \kappa)(u + \gamma)}\right] \tag{9}$$

and using the following inverse Laplace transform,

$$L^{-1}\left[\frac{1}{\sqrt{s - a} + b}\right] = \exp(at)\left[\frac{1}{\sqrt{\pi t}} - b\exp(b^2 t)\,\mathrm{erfc}(b\sqrt{t})\right] \tag{10}$$

we then obtain as a final solution for the signal intensity the following equation:

$$N(t) = \frac{A\exp(-k_f t)}{\gamma}\left[\frac{\gamma}{\gamma - \kappa}\exp(\kappa^2 Dt)\,\mathrm{erfc}(\kappa\sqrt{Dt}) - \frac{\kappa}{\gamma - \kappa}\exp(\gamma^2 Dt)\,\mathrm{erfc}(\gamma\sqrt{Dt})\right] \tag{11}$$

This equation represents a general solution for the above problem and is used in the following work to predict the behavior of the excited state decay curve and hence to obtain the lifetime under different conditions. For the case of infinitely fast heterogeneous kinetics the above equation (11) can be reduced to

$$N(t) = \frac{A}{\gamma}\exp(-k_f t)\exp(\gamma^2 Dt)\,\mathrm{erfc}(\gamma\sqrt{Dt}) \tag{12}$$

in the limit of $\kappa$ tending to infinity. Linearization of the short-time limit of eq 11 gives

$$\ln\left(\frac{N(t)}{A}\right) = -\frac{(\gamma\kappa D\tau_0 + 1)t}{\tau_0} \tag{13}$$

The lifetime with no quencher present, $\tau_0$, is hence related to the apparent rate constant, $\tau$, in the interfacial case by

$$\frac{1}{\tau} = \frac{1}{\tau_0} + \gamma\kappa D = \frac{1}{\tau_0} + \gamma k_{12} c_q \tag{14}$$

which is effectively an interfacial analogue of the standard Stern−Volmer expression, as a plot of the inverse observed lifetime versus quencher concentration should be linear, at least in the short-time domain.

It is worth using the mathematical model developed to explain the failure to observe the occurrence of any heterogeneous quenching in the earlier study[14] with $Ru(bpy)_3^{2+}$. Decay curves were simulated for the conditions corresponding approximately to those found experimentally with the europium ion and $Ru(bpy)_3^{2+}$, respectively, using eq 11, with the quencher concentration set to zero so that the decay was of the conventional exponential form, and eq 12 used to describe the

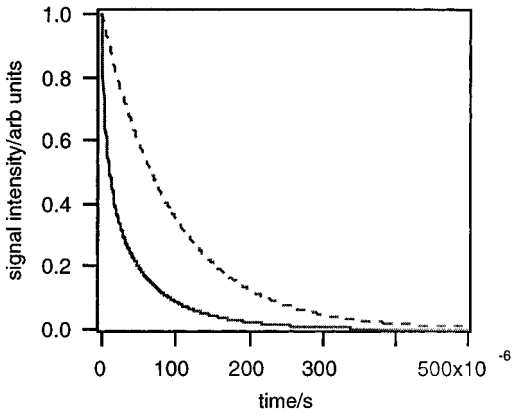


**Figure 3.** Luminescent decay curves with zero (broken line) and infinitely fast (solid line) quenching ($k_q = 0$ and $\infty$) simulated for conditions approximating those of the europium experiments, *viz.* $k_f = 1.04 \times 10^4$ s $^{-1}$, $D = 7.1 \times 10^{-6}$ cm$^2$ s$^{-1}$, and $A = \gamma = 7.69 \times 10^6$ m$^{-1}$.

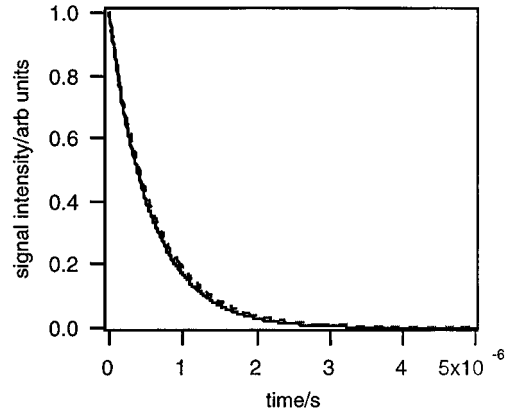


**Figure 4.** Luminescent decay curves with zero (broken line) and infinitely fast (solid line) quenching ($k_q = 0$ and $\infty$) simulated for conditions approximating those of the $Ru(bpy)_3^{2+}$ experiments, *viz.* $k_f = 1.67 \times 10^6$ s $^{-1}$, $D = 3.5 \times 10^{-6}$ cm$^2$ s$^{-1}$, and $A = \gamma = 5.62 \times 10^6$ m$^{-1}$.

limiting case of an infinitely rapid quenching process. The resultant decay curves are shown in Figures 3 and 4. The marked difference in the decay curves between the cases of no and infinitely fast quenching is apparent in Figure 3, implying that quenching with europium would be readily visible. The quenched plot in Figure 4, by contrast, is virtually superimposed on the exponential decay, which suggests that $Ru(bpy)_3^{2+}$ luminescence predominates over quenching as a relaxation pathway and that possible observation of the latter process would require that the interfacial characteristics of the experiment be enhanced.

## Results and Discussion

**Experiments in Homogeneous Solution.** The absorption spectrum of aqueous europium chloride solution is shown in Figure 5. Note particularly that the concentration of europium ion used was 0.1 M and the cell path length was 1 cm; thus the maximum extinction coefficient (at 392.8 nm) is on the order of 1 M$^{-1}$ cm$^{-1}$. The absorption spectrum of anthracene in DCE solution revealed a broad band in the UV, whose tail extended to 395 nm, implying that a relatively significant amount of the excitation beam was absorbed by the anthracene solution. The extinction coefficient at the excitation wavelength was found to be 22.5 M$^{-1}$ cm$^{-1}$, meaning that only around 60% of the incident laser beam was transmitted to the aqueous phase at typical quencher concentrations with the cell geometry em-

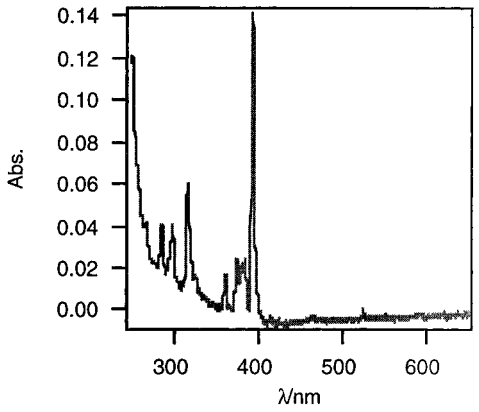


**Figure 5.** Absorption spectrum of a 0.1 M aqueous solution of europium(III) chloride in a 1 cm path length cell.

ployed. However, it should be noted that no quencher luminescence was detected in the region where the europium ion luminescence was monitored.

The quenching of excited state europium ions in homogeneous solution by anthracene has been reported, with acetone as the solvent.[15] Accordingly, preliminary experiments were carried out in acetone with $1 \times 10^{-4}$ M europium solution, with the anthracene concentration being varied over the millimolar range. The luminescent decay of the europium was monitored, as described above, for each anthracene concentration, and an exponential curve fitted to each of the resultant data sets. Standard Stern−Volmer analysis[16] of the resultant luminescent lifetimes as a function of the concentration of anthracene is shown in Figure 6. The gradient of the least-squares straight line gives a value of $6 \times 10^4$ M$^{-1}$ s$^{-1}$ for the homogeneous quenching rate constant, in comparison with the reported[15] value of $1 \times 10^5$ M$^{-1}$ s$^{-1}$, obtained via flash photolysis.

**Experiments with Heterogeneous Systems: Energetics of Transfer.** The quenching process at the liquid−liquid interface was subsequently investigated. Anthracene was chosen as the quencher molecule, as it is reported to be "insoluble" in water.[17] Its partition coefficient between octanol and water has been variously quoted[18] as $3.16 \times 10^4$ and $2.81 \times 10^4$.[19] This coefficient can be extrapolated to the case of the water DCE interface through the following relation:[20]

$$\log P_{oct} = (0.79 \pm 0.13) \log P_{DCE} - (0.26 \pm 0.23) \quad (15)$$

with a correlation coefficient of 0.90. This expression thus allows one to conclude that the partition coefficient of anthracene at the water/DCE interface is between $5 \times 10^5$ and $1 \times 10^6$; thus a millimolar concentration of anthracene in DCE would give rise to an aqueous concentration of anthracene of less than 5 nM.

Similarly, the solubility of a triply charged cation in a salt-free solvent with a relatively low dielectric constant, such as DCE, would normally be low. No luminsescence at 615 nm was noted from DCE in contact with aqueous europium solution. Further, polarization of the ITIES using a standard four-electrode electrochemical cell[1,3] was carried out using a lithium sulfate solution as the aqueous phase and a bis(triphenylphosphoranylidene)−ammonium tetrakis(4-chlorophenyl)borate solution in DCE solution as the organic phase. These electrolytes were chosen to maximize the size of the polarization window that may be obtained at the ITIES. Addition of europium ions did not appear to reduce the size of the potential window, allowing one to conclude that the Gibbs energy of transfer of europium from water to DCE is at least 3 times as large as that of lithium. The Gibbs free energy of transfer of the lithium ion from water

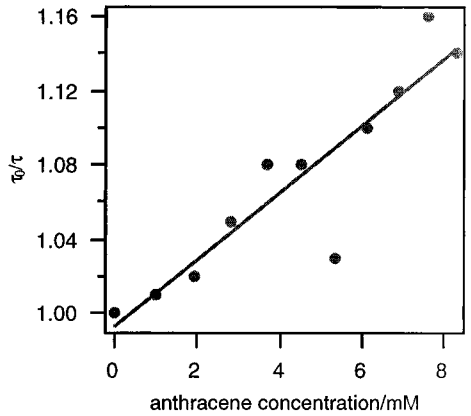


**Figure 6.** Stern−Volmer plot obtained from the luminescent decay of a $1 \times 10^{-4}$ M solution of europium(III) chloride in the presence of anthracene. The experimental points are shown along with a linear regression best fit.

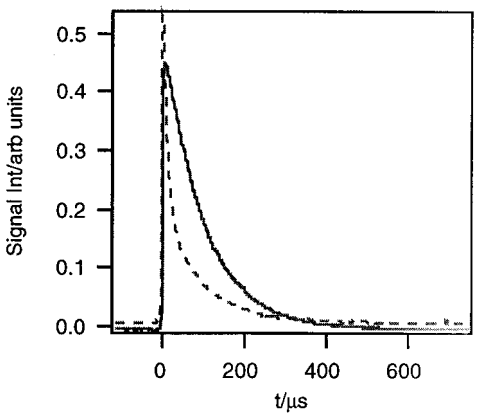


**Figure 7.** Representative experimental decay curves recorded at 615 nm for $5 \times 10^{-3}$ M europium chloride solution in water with (broken line) and without (solid line) a $7 \times 10^{-3}$ M anthracene solution in the adjacent 1,2-DCE phase.

to DCE has been variously quoted[21,22] as being around 57 and 48 kJ $mol^{-1}$, the discrepancies arising from the extra-thermodynamic assumption required to estimate this parameter. On this basis, it may be expected that any interactions noted between anthracene in DCE solution in contact with europium cations in aqueous solution would result from an interfacial process, as the extent of mutual partitioning of the species; hence the chance of homogeneous reactions is extremely low.

**Experiments with Heterogeneous Systems: Treatment of Data.** Experimental data obtained from the system $EuCl_3$(aq)/ /anthracene (1,2-DCE), with no additional supporting electrolyte, were treated in terms of a purely "heterogeneous" quenching model for the reasons outlined in the preceding section: electronically excited europium ions are quenched by electron transfer at the liquid−liquid interface, thus inducing a concentration gradient. The observation of any quenching effect implies that the time scale of diffusion is at least comparable with that of the luminescent process.

A change in the lifetime of the excited state species was predicted to be visible following the addition of a quenching molecule for both the simulated cases detailed in the Theory section. The experimental data obtained using europium and anthracene were analyzed in terms of the mathematical model introduced above for evidence of the proposed quenching. Two representative decay curves, one with and one without quencher, are shown in Figure 7. The data were analyzed in terms of eq 11, with the (known) values of $k_f$, $\gamma$, and $D$ being held constant, and the data fitted in terms of the constant $\kappa$, which is directly

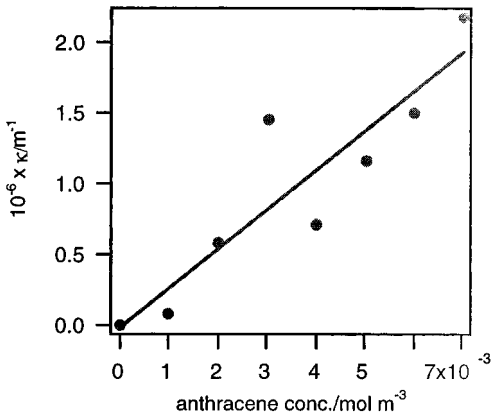


**Figure 8.** Analysis of the experimental decay curves (including those of Figure 7) in terms of eq 12. A linear response is predicted theoretically; a linear regression fit is shown.

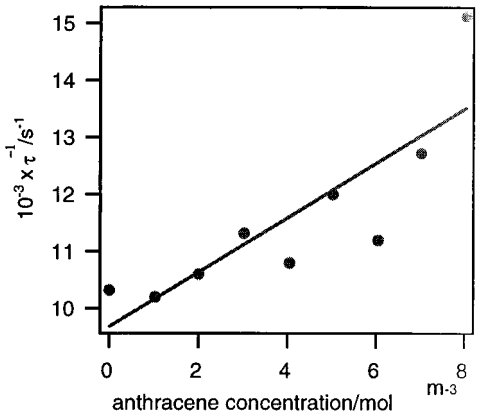


**Figure 9.** Interfacial Stern−Volmer plot obtained from the experimental data presented in another form in Figure 8. The experimental points are shown with the best fit by linear regression.

related to $k_{12}$ (see eq 7). The factor $A$ is the final unknown in this equation, but it is merely a pre-exponential scaling factor, of arbitrary value. Once the $\kappa$ values had been found, they were plotted as a function of the appropriate quencher concentration to produce the graph given in Figure 8, as the definition of $\kappa$ implies that there ought to be a linear relationship between the two parameters. The dependence found experimentally is acceptable and suggests that a quenching process does occur that, for the reasons outlined previously, can be deemed heterogeneous. The experimental data were further analyzed in terms of the interfacial Stern−Volmer expression (eq 14), as the lifetime of the europium ion is long enough to make the Stern−Volmer plot tend toward linearity. The experimental graph is given in Figure 9.

The gradients of the graphs referred to above (Figures 8 and 9) permit the deduction of the second-order interfacial rate constant ($k_{12}$) describing the quenching process. A value of $1.9 \times 10^{-4}$ $m^4$ $mol^{-1}$ $s^{-1}$ (19 $M^{-1}$ cm $s^{-1}$) for $k_{12}$ is found from Figure 8, while Figure 9 permits the deduction of a value of $6.2 \times 10^{-5}$ $m^4$ $mol^{-1}$ $s^{-1}$, however the former value has more validity, as the latter stems from the short-time linearization of the full expression. The bimolecular rate constant can be transformed into a first-order interfacial process, to facilitate comparison with those values measured by electrochemical means for heterogeneous charge transfer processes. Such a transformation requires multiplication by a mean interfacial concentration value of the excess (quencher) species. As the bulk concentration of anthracene used was generally on the order of $5 \times 10^{-3}$ M, then a value of around 0.1 cm $s^{-1}$ is obtained as a pseudo-first-order interfacial rate constant. This kinetic

analysis was performed through consideration of the excited state of europium only and does not allow any conclusions to be drawn about the rate of the back (recombination) reaction. In fact, as the supposed products (the anthracene cation radical and the europium 2+ cation) are of like charges, any back reaction is likely to be negligible. Further, it must be noted that any interfacial electron transfer should be accompanied by an ion transfer process to preserve the electroneutrality of each phase.

## Conclusions

Spectroscopic evidence has been presented for the existence of a photoinduced electron transfer process at the liquid−liquid interface. It has, hitherto, been difficult to probe such rapid processes at this interface using conventional, electrochemical techniques; thus the ability to investigate such events spectroscopically rather than electrochemically is of value. Further the process investigated is of interest as it suggests that photoinduced charge separation occurs at the liquid−liquid, as well as at the semiconductor−liquid, interface.

**Acknowledgment.** R.A.W.D. thanks the Royal Society for a European Exchange Fellowship. Z.D. is indebted to the Commission Fédérale pour les étudiants étrangers for financial support. Laboratoire d'Electrochimie is part of ODRELLI (Organisation, Dynamics and Reactivity at Electrified Liquid/Liquid Interfaces).

## References and Notes

(1) Girault, H. H. *Electrochim. Acta* **1987**, *32*, 383.
(2) Marcus, R. A. *J. Phys. Chem.* **1990**, *94*, 4152.
(3) Girault, H. H.; Schiffrin, D. J. In *Electroanalytical Chemistry*; Bard, A. J. Ed.; Marcel Dekker: New York, 1989; Vol. 15; p 1.
(4) Gerischer, H. *J. Electrochem. Soc.* **1978**, *125*, 218C.
(5) Wei, C.; Bard, A. J.; Mirkin, M. V. *J. Phys. Chem.* **1995**, *99*, 16033.
(6) Fox, M. A. *Adv. Photochem.* **1986**, *13*, 237.
(7) Thomson, F. L.; Yellowlees, L. J.; Girault, H. H. *J. Chem. Soc., Chem. Commun.* **1988**, 1547.
(8) Brown, A. R.; Yellowlees, L. J.; Girault, H. H. *J. Chem. Soc., Faraday Trans. 2* **1993**, *89*, 207.
(9) Marecek, V.; Armond, A. H. D.; Armond, M. K. D. *J. Am. Chem. Soc.* **1989**, *111*, 2561.
(10) Kotov, N. A.; Kuzmin, M. G. *J. Electroanal. Chem.* **1990**, *285*, 223.
(11) Samec, Z.; Brown, A. R.; Yellowlees, L. J.; Girault, H. H. *J. Electroanal. Chem.* **1990**, *288*, 245.
(12) Toriumi, M.; Masuhara, H. *Spectrochim. Acta Rev.* **1991**, *14*, 353.
(13) Sabbatini, N.; Guardigli, M.; Lehn, J.-M. *Coord. Chem. Rev.* **1993**, *123*, 201.
(14) Ding, Z.; Wellington, R. G.; Brevet, P.-F.; Girault, H. H. *J. Phys. Chem.* **1996**, *100*, 10658.
(15) Ermolaev, V. L.; Tachin, V. S. *Opt. Spektrosk.* **1970**, *29*, 93.
(16) Turro, N. J. *Modern Molecular Photochemistry*; University Science Books: Mill Valley, CA, 1991.
(17) *The Merck Index*, 11th ed.; Budavari, S., Ed.; Merck & Co.: Rahway, NJ, 1989.
(18) Sangster, J. *J. Phys. Chem. Ref. Data* **1989**, *18*, 1134.
(19) Hamsch, C.; Fujita, P. *J. Am. Chem. Soc.* **1964**, *86*, 1616.
(20) Steyaert, G.; Lisa, G.; Gaillard, P.; Reymond, F.; Girault, H. H.; Carrupt, P.-A.; Testa, B. *J. Chem. Soc., Faraday Trans.* **1997**, *93*, 401.
(21) Sabela, A.; Marecek, V.; Samec, Z.; Fuoco, R. *Electrochim. Acta* **1991**, *37*, 231.
(22) Shao, Y.; Stewart, A. A.; Girault, H. H. *J. Chem. Soc., Faraday Trans.* **1991**, *87*, 2593.